The minimum distance parametrization of crystal lattices

Gernot J Pauschenwein

Austrian Institute of Technology, Energy Department, Sustainable Thermal Energy Systems, Giefinggasse 2, 1210 Vienna, Austria

E-mail: gernot.pauschenwein@ait.ac.at

Abstract

A general parametrization for all three-dimensional crystal lattices is presented in this paper which guarantees that the three primitive vectors constructed by the parametrization are the three shortest possible, linearly independent lattice vectors existing in the whole lattice. The parameter space of this so-called minimum distance parametrization (MDP) can easily be confined to contain only lattices whose shortest distance between lattice points is not smaller than a given arbitrary length. Together with the also provided extension to general crystal structures the MDP represents a means to parametrize all (and only those) crystal structures allowed for hard core particles.

PACS numbers: 02.40.Dr, 61.46.Hk, 61.50.Ah, 64.70.pv

1. Introduction

To gain an understanding of processes appearing in solids, sound atomic level models for solid structures are necessary. In order to refine existing structural models and even predict new structures computer modelling has become increasingly important, not only in physics but also in biological sciences [1]. Structures, energetics and dynamics of complex materials and molecules are being investigated [2, 3] as well as surface and adsorption phenomena [4], mineral interfaces [5] and defects [6].

There exist different ways of theoretical investigation. Molecular dynamics represents a straightforward tool for finding equilibrium structures through amorphization and recrystallization (see e.g. [7]). This method is also suitable to investigate glassy states [8, 9] and even dynamic effects, like oriented aggregation [10]. Nevertheless, its main disadvantages are the high computational cost and short simulation times (in the order of nanoseconds), which make it inefficient in the task of determining a full phase diagram. Another, more random-based simulation method is Monte Carlo simulation (see applications to phase detection e.g. in [3, 11, 12]), but still the computational cost is high.

An alternative to simulation is to use experimental results or simple point-by-point variations to obtain the structural parameters for which the energies of the corresponding solids are then calculated. These competing structures then yield the stable structures in the phase diagram, e.g. for boric oxide [13]. It is also possible to select candidate structures randomly which are then energetically refined, applied for example to scrutinize the metallization of aluminium hydride at high pressure [14].

In an effort to obtain an efficient means to generate candidate structures for drawing phase diagrams, evolutionary algorithms have been adopted for structural optimization recently. Especially in hard matter investigations [15–17] it became clear that a Lamarckian genetic algorithm (L-GA), where each individual is (locally) optimized or relaxed before reproduction, is advantageous as compared to pure Darwinian genetic algorithms (D-GA), where relaxation is applied only to the final candidate structure provided by the algorithm [18]. This technique also led to the theoretical prediction of experimentally verified previously unknown phases, especially at high pressure, e.g. phase III of solid hydrogen [19], an ionic crystal phase of ammonia [20], metallic structures of oxygen [21], new structures for lithium, potassium and rubidium [22], a wide bandgap dielectric of pure sodium [23] and new phases of boron [24] and nitrogen [25]. Also, the design of new superconductors could be enabled through the better understanding of the relations between structure and superconductivity from, on the one hand, newly detected superconducting structures [26–28] or, on the other hand, the loss of superconductivity under pressure [29].

Also in soft matter a promising tool to accomplish the problem of predicting equilibrium crystal structures is a genetic-algorithm-based search strategy, although so far only the method of a D-GA has been used [11, 12, 30–36], where all operations (mutation, cross-over) are only performed on the genotype, none on the phenotype (for an explanation see again [18]).

Common to all theoretical tools (except molecular dynamics and investigations of glasses) is that each candidate structure, whether proposed randomly, by experiment, intuition, or a kind of GA, can be described by a crystal structure and the positions of basis particles in the unit cell. Thus, the *complete* pool of candidate structures can be parametrized through all possibilities for the three primitive lattice vectors together with a prescription for the positions of the basis particles. Obviously there exist a lot of ambiguities, since the same structure can be described in principle by infinitely many possibilities for the primitive unit cell. Even if ambiguities represent no problem for the optimization algorithm of choice, in general the larger the parameter space the slower will be the convergence. Hence it would be favourable to remove as many ambiguities as possible from parameter space. In addition, when considering hard core particles, the standard parametrization for the three primitive vectors using, e.g., three length and three angle parameters can severely spoil the convergence of a GA: it has turned out [34, 35] that it is highly preferential if all configurations where the shortest particle distance is smaller than the hard core diameter are excluded from parameter space *a priori*.

Therefore, the aim of this paper is to explain how to set up a pool of crystal structures for particles with a hard core diameter σ that does not contain structures with overlapping cores. The major step in achieving this is to find a parametrization of crystal structures where the smallest possible distance between two hard sphere particles in the whole crystal is one of the parameters and can hence be confined. It has become clear that the main issue was to solve this problem for the underlying Bravais lattice, i.e. to find a parametrization which provides the possibility of restricting the shortest distance between *lattice points* to lie above a certain minimum value. The resulting parametrization shall be called 'minimum distance parametrization' (MDP). In this parametrization also most ambiguities in parameter space will be removed (the remaining ones represent a measure-zero set in parameter space), as is described in more detail elsewhere [37].

In the following section, an explanation of the MDP is given through a constructive proof of existence for all crystal lattices. In section 3, the whole parameter space of the MDP is constructed while in section 4 the MDP for the cubic Bravais lattices is described as an example. Finally, the extension to general crystals is given before some concluding remarks.

2. Existence of the MDP

Considering an arbitrary crystal lattice, it is straightforward to identify the smallest distance between lattice points: there obviously exists a length δ that is small enough to guarantee that there lies only one lattice point inside a sphere of radius δ and centre at an arbitrary lattice point **P** (the only lattice point inside the sphere), denoted by $S_{\mathbf{P}}(\delta)$. One can then gradually increase the radius of this sphere until at least one other lattice point is contained in the surface of the sphere, the corresponding radius s being then the smallest distance between lattice points. While s is uniquely defined, there might be several vectors $\mathbf{s}_i$ from **P** to lattice points at the surface of the sphere $S_{\mathbf{P}}(s)$ that satisfy $|\mathbf{s}_i| = s$.

Now choose one of the $\mathbf{s}_i$ arbitrarily and call it **c**. (There are at least always two possibilities, since if **c** is a lattice vector so is $-\mathbf{c}$.) If there exists another vector in the set of $\mathbf{s}_i$ that is *linearly independent* of **c**, call it **b**. Else, further increase the diameter of the sphere, until at least one other lattice point happens to lie on the spherical surface and the following condition is met: the lattice vector from **P** to a lattice point at the surface is linearly independent of **c**. Again, it is possible that several vectors of the same magnitude fulfil this requirement; one of them shall be called **b**. In the same manner one can construct a third lattice vector **a**, which of course must not lie in plane with **b** and **c**. It may even happen (e.g. for cubic lattices, see section 4) that already in the first set of the $\mathbf{s}_i$ there are three linearly independent vectors, i.e. the three primitive vectors **c**, **b**, and **a** are of equal length.

As has thus been demonstrated, it is always possible to construct a primitive unit cell of a given crystal lattice where the primitive vectors **c**, **b**, and **a** are the three shortest possible, linearly independent lattice vectors, satisfying

$$c \leqslant b \leqslant a \tag{1}$$

(using $|\mathbf{a}| = a$, $|\mathbf{b}| = b$ and $|\mathbf{c}| = c$). As a consequence, it is sufficient for a general parametrization of all lattices to find a parametrization for all possible triplets of vectors that satisfy condition (1) and for which the quantity

$$L(k, m, n) = |k\mathbf{a} + m\mathbf{b} + n\mathbf{c}|, \tag{2}$$

fulfils for all $(k, m, n) \in \mathbb{Z}^3$

$$L(k \neq 0, m, n) \geqslant a, \tag{3}$$

$$L(0, m \neq 0, n) \geqslant b \quad \text{and} \tag{4}$$

$$L(0, 0, k) \geqslant c. \tag{5}$$

It is important to note that one *does not* need an unambiguous parametrization; it is satisfactory just to include all possible structures. To make the parameter space as small as possible and hence improve the convergence e.g. of a genetic algorithm, it is nevertheless convenient if ambiguities are most widely excluded.

3

3. Construction of the parameter space of the MDP

W.l.o.g. the following representation is chosen for the three primitive vectors, automatically satisfying conditions (1) and (5), in a Cartesian basis:

$$\mathbf{c} = c \begin{pmatrix} 1 \\ 0 \\ 0 \end{pmatrix}, \quad \mathbf{b} = cp \begin{pmatrix} \cos\varphi \\ \sin\varphi \\ 0 \end{pmatrix} \quad \text{and} \quad \mathbf{a} = cpq \begin{pmatrix} \xi \\ \eta \\ \zeta \end{pmatrix}, \tag{6}$$

with

$$0 < c, \tag{7}$$

$$1 \leqslant p, q \quad \text{and} \tag{8}$$

$$1 = \sqrt{\xi^2 + \eta^2 + \zeta^2}. \tag{9}$$

Some ambiguities (including the one of mirrored crystals, which usually have equal properties) can be excluded by demanding

$$0 < \varphi \leqslant \frac{\pi}{2}, \tag{10}$$

$$\eta \begin{cases} \geqslant 0 & \xi \geqslant 0 \\ > 0 & \xi < 0 \end{cases}, \tag{11}$$

$$\zeta > 0. \tag{12}$$

Note that for most numerical optimization algorithms it would be beneficial to include the rim of allowed structures, i.e. demand only $\eta \geqslant 0 \; \forall \xi$ instead of inequalities (11). The reason for the parametrization of $\mathbf{a}$ using the Cartesian components ξ, η, and ζ instead of two independent angles will become clear at the end of the following constructive derivation of the MDP.

From equations (6) one recognizes that c is a prefactor for all the three primitive vectors, and hence represents just a scaling factor for the whole lattice. Therefore, the aim is now to identify a subspace of the five parameters p, q, φ, ξ and η in $\mathbb{R}^5$ (the positive parameter ζ follows from equation (9)), so that conditions (3) and (4) are obeyed, too. This task will be performed in two steps: first considering the plane spanned by $\mathbf{c}$ and $\mathbf{b}$ (i.e. condition (4)); second, taking also the third shortest vector (i.e. condition (3)) into consideration.

3.1. The c–b lattice plane

The two primitive vectors $\mathbf{c}$ and $\mathbf{b}$ define a 2D lattice, a so-called *lattice plane* of the 3D lattice. To guarantee condition (4), consider a lattice line parallel to $\mathbf{c}$ and passing through a lattice point $\mathbf{P}$ (see figure 1). The condition that out of all lattice vectors in the 2D lattice that are linearly independent of $\mathbf{c}$, $\mathbf{b}$ is the shortest one results in the restriction that there must not be any lattice points having distances shorter than b from $\mathbf{P}$, with the possible exception of those at $\mathbf{P} + n\mathbf{c}$, $n \in \mathbb{Z}$, lying on the same lattice line as $\mathbf{P}$ (c is allowed to be shorter than b). This has especially to hold for all points of the adjacent lattice line, which can be constructed by adding $\mathbf{b}$ to each point of the lattice line that includes $\mathbf{P}$ (see figure 1).

Calculation of the distances between $\mathbf{P}$ and the lattice points of the adjacent $\mathbf{c}$-line gives $\sqrt{b^2 - 2cnb\cos\varphi + n^2c^2}$, $n \in \mathbb{Z}$. From condition (10) it follows that $\cos\varphi \geqslant 0$; therefore, only non-negative values of n have to be checked to guarantee that this distance is larger
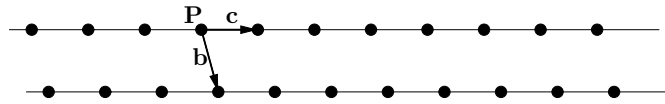
Figure 1. Two adjacent lattice lines in the **c** direction.

than or equal to b. For convenience define a function $f(n)$, which is the square of the above expression, i.e. the square of the calculated distances,

$$f(n) = b^2 - 2cnb \cos \varphi + n^2 c^2, \tag{13}$$

which has to be larger than or equal to b^2 for all values of n. $f(n)$ is obviously a convex parabola with apex at $n_{\min} = \frac{b}{c} \cos \varphi \geqslant 0$, and of course $f(0) = b^2$. The condition $f(1) \geqslant b^2$ leads to[1]

$$\cos \varphi \leqslant \frac{c}{2b} = \frac{1}{2p}, \tag{14}$$

which results in $n_{\min} \leqslant 1/2$. Since the minimum of the parabola therefore lies between 0 and 1 (the two points where $f(n) \geqslant b^2$ already holds), it immediately follows that $f(n) > b^2, \forall n > 1$.

Lattice points residing in the next but neighbouring lattice line always have a distance larger than b provided that inequality (14) holds, which may be shown as follows. Let the distance between neighbouring **c**-lines be d; hence all distances to lattice points of the next but neighbouring lattice line are greater than or equal to $2d$. d is minimal if the equality sign in (14) is valid, i.e. $\sqrt{d^2 + c^2/4} = b$. Therefore,

$$2d \geqslant b\sqrt{4 - c^2/b^2} \geqslant \sqrt{3}b > b, \tag{15}$$

and analogously it follows that lattice points in the mth neighbouring lattice line ($m > 2$) have a larger distance than b from **P**.[2]

Therefore, inequality (14) is the only necessary condition to guarantee that **b** and **c** are the shortest, linearly independent 2D lattice vectors with $c \leqslant b$ in the 2D lattice described by these two vectors as primitive ones.

3.2. Constructing **a** as the third shortest lattice vector

Obviously, like for p, all values for $q \geqslant 1$ have to be attainable; restrictions will hence only affect the parameters defining the direction of **a**. Since $\zeta, \eta \geqslant 0$ and $\varphi \leqslant \pi/2$ (inversion and mirror symmetry), (3) can be reduced to

$$|k \cdot \mathbf{a} - (m\mathbf{b} + n\mathbf{c})| \geqslant a \qquad \forall k, m, n \in \mathbb{Z} : m \geqslant 0, k \geqslant 1. \tag{16}$$

First consider the case $k = 1$. To visualize the remaining conditions construct a 'mogul slope', defined by spheres of radius a with centres at the lattice points of the **b**–**c** lattice plane (see figure 2). According to condition (16), the vector **a** must point above this mogul slope. Since **a** has the same length as the radius of the spherical moguls, this restricts the apex of **a** to the spherical, upper cap of the region enlarged in figure 3. It will become clear that of this infinitely extended mogul slope only the four closest moguls are important, i.e. if **a** points above these four, it also points above any other one. Hence the distances of the lattice point **a**

---

[1] Note that $\sqrt{f(1)}$ is the length of the shorter diagonal of the parallelogram spanned by **b** and **c**.
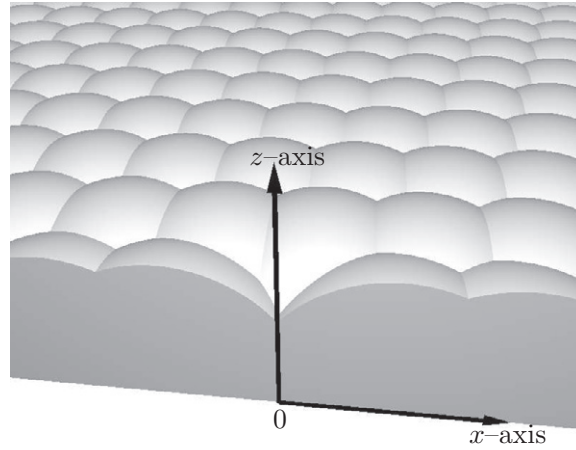[2] Due to inversion symmetry $m \leqslant -1$ need not be checked.

Figure 2. The 'mogul slope' defined by spheres of radius a around the lattice points of the **c**–**b** lattice plane in the positive y-half plane. The y-axis, obtained via $\hat{\mathbf{y}} = \hat{\mathbf{z}} \times \hat{\mathbf{x}}$, cannot be seen (hats indicate unit vectors in the corresponding directions).

from the four lattice points $\pm\mathbf{c}$, $\mathbf{b}$ and $\mathbf{b} - \mathbf{c}$ are accounted for. From basic manipulations and usage of (9) it follows that

$$|\mathbf{a} - \mathbf{c}| \geqslant cpq \Rightarrow \xi \leqslant \frac{1}{2pq}, \tag{17}$$

$$|\mathbf{a} + \mathbf{c}| \geqslant cpq \Rightarrow \xi \geqslant -\frac{1}{2pq}, \tag{18}$$

$$|\mathbf{a} - \mathbf{b}| \geqslant cpq \Rightarrow \xi \cos\varphi + \eta \sin\varphi \leqslant \frac{1}{2q}, \quad \text{and} \tag{19}$$

$$|\mathbf{a} - \mathbf{b} + \mathbf{c}| \geqslant cpq \Rightarrow \xi(p\cos\varphi - 1) + \eta p \sin\varphi \leqslant \frac{p^2 + 1 - 2p\cos\varphi}{2pq}. \tag{20}$$

In the ξ–η parameter space, this region, obtained by projecting the allowed region for $\mathbf{a}$ onto the x–y plane and scaling the resulting region by $1/(pq)$, describes the Wigner–Seitz unit cell (WSC, in the positive ξ half-plane) of a 2D lattice described by $\frac{n}{cpq}\mathbf{c} + \frac{m}{cpq}\mathbf{b}$ ($n \in \mathbb{Z}, m \in \mathbb{Z}_0^+$), i.e. the **b**–**c** lattice plane scaled by the inverse length of $\mathbf{a}$ (see figure 4). Analytically, this is described by the right-side inequalities (17)–(20). The set of all possibilities for ξ and η is easily parametrized for these Cartesian coordinates; in terms of p, φ and q one obtains

$$-\frac{1}{2pq} \leqslant \xi \leqslant \frac{1}{2pq}, \tag{21}$$

$$\left. \begin{array}{ll} \xi < 0: & 0< \\ \xi \geqslant 0: & 0\leqslant \end{array} \right\} \eta \leqslant \begin{cases} \dfrac{p^2 + 1 - 2p\cos\varphi}{2p^2q\sin\varphi} + \xi\dfrac{1 - p\cos\varphi}{p\sin\varphi}, & \xi \leqslant \dfrac{2p\cos\varphi - 1}{2pq} \\[3mm] \dfrac{1}{2q\sin\varphi} - \xi\cot\varphi, & \xi > \dfrac{2p\cos\varphi - 1}{2pq}, \end{cases} \tag{22}$$
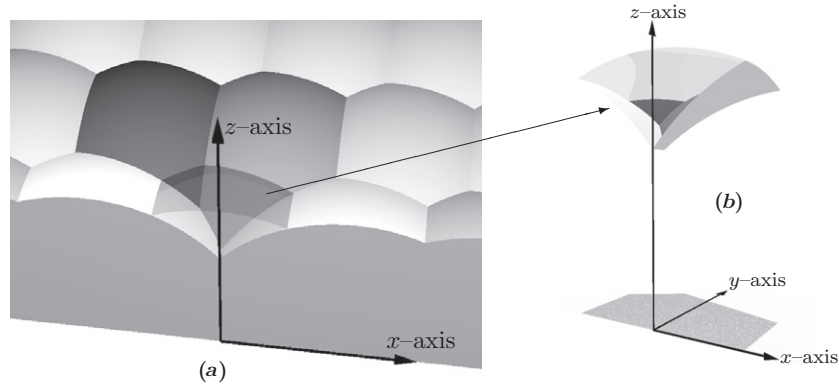
where ζ finally follows from (9).

Figure 3. The mogul slope, similar to figure 2, is drawn, but with the four relevant moguls for the vector **a**, described by the left-side equations (17)–(20) (with '$\geqslant$' replaced by '='), shaded in different grey scales in (*a*). The allowed regime for **a** is the spherical upper cap of the transparent, pendentive like region, enlarged in (*b*), where also the projection onto the *x*–*y* plane is shaded in grey.
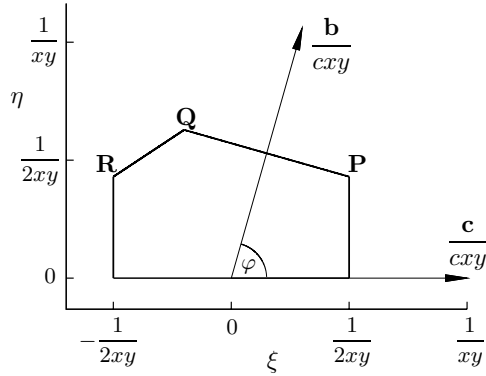

Figure 4. The allowed pentagonal region of ξ and η for example values of $p = 1.1$, $\varphi = 1.29$, and $q = 1.2$. The points **P**, **Q** and **R** are given in the text.

To understand that the four accounted for moguls are already sufficient to guarantee inequality (16) for $k = 1$ consider again the **b**–**c** lattice plane. The projection of **a** lies, by construction, inside (or at the rim of) the 2D WSC around the origin. The projection of any other lattice point of the lattice plane shifted by **a** hence lies outside (or also at the rim of) this WSC. Hence, the projected point closest to the lattice point at the origin is the one of **a** (or more of equal distance, if **a** lies at the rim). But the shortest distance between lattice points of neighbouring lattice planes is just the square root of the sum of the squares of the plane distance and the distance to the closest projected lattice point.

The proof that also the distances to lattice points of non-neighbouring lattice planes are greater than a, i.e. inequality (16) for $k > 1$, works similar to the one for the lattice lines in section 3.1. The distance between neighbouring **c**–**b** lattice planes is $cpq\zeta$. On the pendentive cap, the smallest value of ζ is obtained at the corner points labelled as **P**, **Q**, and **R** in figure 4

since the rims are parts of circles with centres in the x–y plane. The ξ, η, and ζ coordinates of these points are given by

$$\mathbf{P} = \left(\frac{1}{2pq}, \frac{p - \cos\varphi}{2pq\sin\varphi}, \frac{\sqrt{4\sin^2\varphi p^2 q^2 - p^2 + 2p\cos\varphi - 1}}{2pq\sin\varphi} \right), \tag{23}$$

$$\mathbf{Q} = \left(\frac{2p\cos\varphi - 1}{2pq}, \frac{(1 - 2\cos^2\varphi)p + \cos\varphi}{2pq\sin\varphi}, \frac{\sqrt{4\sin^2\varphi p^2 q^2 - p^2 + 2p\cos\varphi - 1}}{2pq\sin\varphi} \right) \quad \text{and} \tag{24}$$

$$\mathbf{R} = \left(-\frac{1}{2pq}, \frac{p - \cos\varphi}{2pq\sin\varphi}, \frac{\sqrt{4\sin^2\varphi p^2 q^2 - p^2 + 2p\cos\varphi - 1}}{2pq\sin\varphi} \right), \tag{25}$$

i.e. they have equal ζ components. The distance to lattice points in non-neighbouring (and different) lattice planes is always greater than or equal to $2cpq\zeta$. Inserting the smallest possible ζ from above and demanding $2cpq\zeta \geqslant a = cpq$ leads to

$$3p^2 q^2 \sin^2\varphi - p^2 + 2p\cos\varphi - 1 \geqslant 0. \tag{26}$$

The left-hand side (l.h.s.) of this inequality is smallest (w.r.t. q) if $q = 1$, and expressing all φ dependences in terms of $\cos\varphi$, one obtains

$$-3p^2 \cos^2\varphi + 2p\cos\varphi + 2p^2 - 1 \geqslant 0. \tag{27}$$

This l.h.s. is a concave parabola in $\cos\varphi$, the minimum value w.r.t. $\cos\varphi$ is hence reached at one (or both) of the boundaries of this variable, i.e. $\cos\varphi = 0$ and $\cos\varphi = 1/(2p)$. In both cases inequality (27) is true because of $p \geqslant 1$.

3.3. Summary

To summarize, the whole parameter space to describe all crystal lattices through the primitive vectors defined by equations (6) is given by

$$c, p, q, \varphi, \xi, \eta, \zeta \in \mathbb{R} \tag{28}$$

with

$$c > 0, \tag{29}$$

$$p \geqslant 1, \tag{30}$$

$$0 \leqslant \cos\varphi \leqslant \frac{1}{2p}, \tag{31}$$

$$q \geqslant 1, \tag{32}$$

$$-\frac{1}{2pq} \leqslant \xi \leqslant \frac{1}{2pq}, \tag{33}$$

$$0 < \eta \leqslant \frac{p^2 + 1 - 2p\cos\varphi}{2p^2 q \sin\varphi} + \xi\frac{1 - p\cos\varphi}{p\sin\varphi} \quad \text{if} \quad \xi \leqslant \frac{2p\cos\varphi - 1}{2pq}, \tag{34}$$

$$0 < \eta \leqslant \frac{1}{2q\sin\varphi} - \xi\cot\varphi \quad \text{if} \quad \frac{2p\cos\varphi - 1}{2pq} < \xi < 0, \tag{35}$$

$$0 \leqslant \eta \leqslant \frac{1}{2q\sin\varphi} - \xi\cot\varphi \quad \text{if} \quad \xi \geqslant 0 \quad \text{and} \tag{36}$$

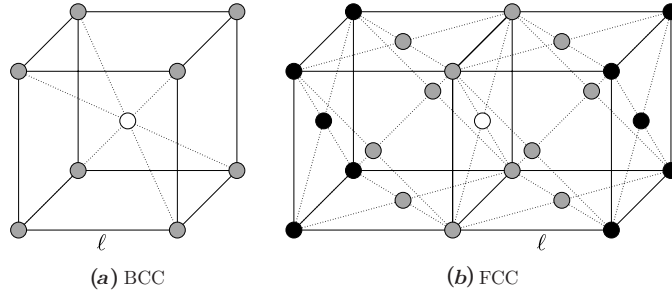$$\zeta = \sqrt{1 - \xi^2 - \eta^2}. \tag{37}$$

Figure 5. (*a*) The conventional BCC cell with edge length ℓ. The distances from the white particle to the grey ones (the eight nearest neighbours) are all the same and equal to $\ell\sqrt{3}/2$. (*b*) Two adjacent conventional FCC cells with edge length ℓ. The distances from the white particle to the grey ones (the 12 nearest neighbours) are all the same and equal to $\ell/\sqrt{2}$.

4. A simple example: the cubic Bravais lattices in the MDP

Let the side length of the conventional cubic unit cell be ℓ. To find out the MDP parameters for the cubic lattices start with the simplest case, which is the *simple cubic* (SC) lattice. It is easy to recognize that all the three MDP vectors have equal lengths: the nearest neighbour distance ℓ. The correspondence between the MDP parameters and the conventional parameter ℓ for the SC lattice is hence given by

$$c = \ell \wedge p = q = 1 \wedge \varphi = \frac{\pi}{2} \wedge \xi = \eta = 0 \wedge \zeta = 1. \tag{38}$$

It is usually very helpful for an understanding of the MDP parametrization to visualize the actual situation in the ξ–η plane. The very simple SC case is depicted in figure 6(*a*).

The case of the *body centred cubic* (BCC) lattice is visualized in figure 5(*a*), where the conventional BCC unit cell is drawn. It is again possible to select three linearly independent primitive vectors pointing to nearest neighbours. Due to the restrictions of the MDP (inequalities (31), (33)–(36)) there remains only one possibility:

$$c = \ell\sqrt{3}/2 \wedge p = q = 1 \wedge \varphi = \arccos\left(\frac{1}{3}\right) \wedge$$
$$\xi = -\frac{1}{3} \wedge \eta = \frac{\sqrt{2}}{3} \wedge \zeta = \sqrt{\frac{2}{3}}, \tag{39}$$

shown in the ξ–η plane in figure 6(b).

In the case of the *face centred cubic* (FCC) lattice, visualized in figure 5(*b*), the ambiguities are not completely reduced by conditions (31), (33)–(36). After choosing the vector **c** as one arbitrary vector out of the 12 pointing to the nearest neighbours of one lattice point, there remain two possibilities for the choice of **b**: one enclosing an angle of $\pi/3$ with **c** and another one perpendicular to **c**. For the third vector, **a**, also of the same length as **c** and **b**, there are again multiple possibilities in each case, which can be summarized as follows:

$$c = \ell/\sqrt{2} \wedge p = q = 1 \wedge$$
$$\begin{cases} \varphi = \frac{\pi}{2} \wedge \zeta = \frac{1}{\sqrt{2}} \wedge \eta = \frac{1}{2} \wedge \xi = \pm\frac{1}{2} \\ \varphi = \frac{\pi}{3} \wedge \zeta = \sqrt{\frac{2}{3}} \wedge \begin{cases} \eta = \frac{1}{2\sqrt{3}} \wedge \xi = \pm\frac{1}{2} \\ \eta = \frac{1}{\sqrt{3}} \wedge \xi = 0, \end{cases} \end{cases} \tag{40}$$

(a) SC (square)   *(b)* BCC (special centred rectangular with $\cos\varphi = \frac{1}{3}$)   *(c)* FCC (squared)   *(d)* FCC (hexagonal)
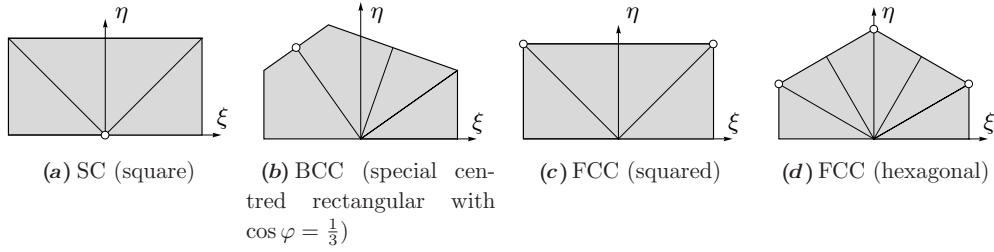
Figure 6. Projection of the pendentive cap like in figure 4 and the points for **a** (white) to describe the corresponding lattices as labelled in the subcaptions. The 2D symmetry of the **b**–**c** lattice plane is given in parenthesis. (*a*) SC (square), (*b*) BCC (special centred rectangular with $\cos\varphi = \frac{1}{3}$), (*c*) FCC (squared), (*d*) FCC (hexagonal).

where the curly bracket stands for an 'or' composition of the enclosed lines. All sets of parameters are again visualized in the $\xi-\eta$ plane in figures 6(*c*) and (*d*).

In the panels for the FCC cases in figure 5 it is also observable that if only one of the allowed points for **a** was provided (for given p, q and φ), the symmetry operations of the underlying 2D lattice would generate all remaining ones. This fact turns out to be the case also for all other Bravais lattices, as is shown elsewhere [37]. However, except for highly symmetric lattices (e.g. the FCC lattice), there can be different points in such a $\xi-\eta$ plot that represent the MDP for the same lattice and are not linked by a simple 2D symmetry operation.

5. More than one basis particle

The main concern is of course to find the smallest distance occurring in a complete crystal, i.e. when the lattice *and* the positions of the basis particles are considered. The discussion here only includes structures of equally sized hard sphere particles, but the extension to basis particles of different diameters should be straightforward.

For one additional basis particle (one is always positioned at the lattice points) one only has to check which distance in the unit cell is the shortest one. The position vector for the additional basis particle is

$$\mathbf{v}_2 = v_{2a}\mathbf{a} + v_{2b}\mathbf{b} + v_{2c}\mathbf{c} \tag{41}$$

with $v_X \in [0, 1)$. One of the distances

$$
\begin{aligned}
&|\mathbf{c}|, \\
&|\mathbf{v}_2|, \qquad\quad |\mathbf{v}_2 - \mathbf{c}|, \\
&|\mathbf{v}_2 - \mathbf{a}|, \qquad |\mathbf{v}_2 - \mathbf{a} - \mathbf{c}|, \\
&|\mathbf{v}_2 - \mathbf{b}|, \qquad |\mathbf{v}_2 - \mathbf{b} - \mathbf{c}|, \\
&|\mathbf{v}_2 - \mathbf{a} - \mathbf{b}| \quad \text{or} \quad |\mathbf{v}_2 - \mathbf{a} - \mathbf{b} - \mathbf{c}|
\end{aligned} \tag{42}
$$

is the shortest one.

For more than one additional basis particle their positions are given by

$$\mathbf{v}_i = v_{ia}\mathbf{a} + v_{ib}\mathbf{b} + v_{ic}\mathbf{c}, \qquad i = 2, 3, \ldots \tag{43}$$

and, in addition to (42), for each i one has to check the distances between the additional basis particles themselves. For this also the $3 \times 3 \times 3 - 1$ adjacent unit cells have to be considered. One finally arrives at the shortest distance $d_{\min}$ as a function of the crystal parameters $p, \varphi, q,$

ξ, η, $\{v_{iX}\}$ and c as an overall scaling factor, i.e. $d_{\min} = cd^{\star}_{\min}(p, \varphi, q, \xi, \eta, \{v_{iX}\})$. Hence it is possible to delimit the c-values in terms of the other crystal parameters in a way that the shortest distance cannot obtain lengths below a chosen minimum, e.g. the diameter σ of the spherical hard core particles. Defining

$$c_{\min} = \frac{\sigma}{d^{\star}_{\min}(p, \varphi, q, \xi, \eta, \{v_{iX}\})} \tag{44}$$

inequality (29) can be replaced by

$$c \geqslant c_{\min}, \tag{45}$$

and together with the restrictions (30)–(37) the parametrization of all crystal structures for equally sized hard sphere particles is complete.

Note however that, although strong evidence exists [34–36] through billions of randomly generated crystals with up to 29 basis particles, which were subsequently 'evolved' through hundreds of 'generations' using a genetic algorithm and finally optimized for lowest enthalpy using Powell's method [38], that the presented parametrization indeed provides the shortest occurring distance between particles of the parametrized crystal, an exact proof for the possibility of this limitation to 27 unit cells has still to be done.

6. Conclusion

The MDP provided by equations (29)–(37) parametrizes all crystal lattices through the three primitive lattice vectors given by (6). These vectors always represent the three shortest possible, linearly independent lattice vectors, and they are ordered by magnitude according to $a \geqslant b \geqslant c$. Both assertions have been proven in section 3. The extension of the MDP from lattices to whole crystals is also given completely (without proof), i.e. all crystal structures are incorporated.

Thus, the MDP can be easily used to exclude crystal structure configurations with overlaps of hard core particles from parameter space. The remaining parameter region can, for given number of basis particles n, be mapped to a $(3n + 3)$-dimensional hypercube, if the shortest particle distance in the crystal is confined to be at longest equal to the cutoff distance of the interaction potential, see [37] for further details.

References

[1] Catlow C R A, Bell R G and Slater B 2004 Static lattice modelling and structure prediction of micro- and mesoporous materials *Computer Modelling of Microporous Materials* ed C R A Catlow, R A van Santen and B Smit (London: Academic) pp 1–24
[2] Catlow C R A 1997 Need and scope of modelling techniques *Computer Modeling in Inorganic Crystallography* ed C R A Catlow (London: Academic) pp 1–22
[3] Glaser M A, Grason G M, Kamien R D, Košmrlj A, Santangelo C D and Ziherl P 2007 Soft spheres make more mesophases *Europhys. Lett.* **78** 46004

[4] Kundu T K, Rao K H and Parker S C 2006 Atomistic simulation studies of magnetite surface structures and adsorption behavior in the presence of molecular and dissociated water and formic acid *J. Colloid Interface Sci.* **295** 364–73

[5] Parker S C, Cooke D J, Marmier A, Martin P, Spagnoli D, Sayle D C and Watson G W 2006 Modelling structure and transport at mineral interfaces at the atomic level *Geochim. Cosmochim. Acta* **70 (Suppl. 1)** A471

[6] Ye F, Mori T, Ou D R, Cormack A N, Lewis R J and Drennan J 2008 Simulation of ordering in large defect clusters in gadolinium-doped ceria *Solid State Ion.* **179** 1962–7

[7] Sayle T X T, Catlow C R A, Maphanga R R, Ngoepe P E and Sayle D C 2006 Evolving microstructure in MnO$_2$ using amorphisation and recrystallisation *J. Cryst. Growth* **294** 118–29 (New Advances in Crystal Growth and Nucleation—a collection of papers contributed by the members of the UK Network of Crystal Growth and Nucleation of Complex Materials or presented at the 2005 Summer School on Crystal Growth and Nucleation of Complex Materials, New Advances in Crystal Growth and Nucleation)

[8] Du J and Cormack A N 2005 The structure of erbium doped sodium silicate glasses *J. Non-Cryst. Solids* **351** 2263–76

[9] Takada A, Richet P, Catlow C R A and Price G D 2008 Molecular dynamics simulation of temperature-induced structural changes in cristobalite, coesite and amorphous silica *J. Non-Cryst. Solids* **354** 181–7 (Physics of Non-Crystalline Solids 11, 11th International Conference on the Physics of Non-Crystalline Solids)

[10] Spagnoli D, Banfield J F and Parker S C 2008 Free energy change of aggregation of nanoparticles *J. Phys. Chem.* C **112** 14731–6

[11] Mladek B M, Gottwald D, Kahl G, Neumann M and Likos C N 2006 Formation of polymorphic cluster phases for a class of models of purely repulsive soft spheres *Phys. Rev. Lett.* **96** 045701

[12] Mladek B M, Gottwald D, Kahl G, Neumann M and Likos C N 2006 Erratum: Formation of polymorphic cluster phases for a class of models of purely repulsive soft spheres [Phys. Rev. Lett. 96, 045701 (2006)] *Phys. Rev. Lett.* **97** 019901

[13] Takada A, Catlow C R A, Price G D and Hayward C L 1997 Periodic *ab initio* Hartree–Fock study of trigonal and orthorhombic phases of boric oxides *Phys. Chem. Miner.* **24** 423–31

[14] Pickard C J and Needs R J 2007 Metallization of aluminum hydride at high pressures: a first-principles study *Phys. Rev.* B **76** 144114

[15] Woodley S M, Battle P D, Gale J D and Catlow C R A 1999 The prediction of inorganic crystal structures using a genetic algorithm and energy minimisation *Phys. Chem. Chem. Phys.* **1** 2535–42

[16] Oganov A R and Glass C W 2006 Crystal structure prediction using *ab initio* evolutionary techniques: principles and applications *J. Chem. Phys.* **124** 244704

[17] Oganov A R and Glass C W 2008 Evolutionary crystal structure prediction as a tool in materials design *J. Phys.: Condens. Matter* **20** 064210

[18] Woodley S M and Catlow C R A 2009 Structure prediction of titania phases: implementation of Darwinian versus Lamarckian concepts in an evolutionary algorithm *Comput. Mater. Sci.* **45** 84–95 (Selected papers from the E-MRS 2007 Fall Meeting Symposium G: Genetic Algorithms in Materials Science and Engineering—GAMS-2007

[19] Pickard C J and Needs R J 2007 Structure of phase III of solid hydrogen *Nat. Phys.* **3** 473–6

[20] Pickard C J and Needs R J 2008 Highly compressed ammonia forms an ionic crystal *Nat. Mater.* **7** 775–9

[21] Ma Y, Oganov A R and Glass C W 2007 Structure of the metallic zeta-phase of oxygen and isosymmetric nature of the epsilon-zeta phase transition: *ab initio* simulations *Phys. Rev.* B **76** 064101

[22] Ma Y, Oganov A R and Xie Y 2008 High-pressure structures of lithium, potassium, and rubidium predicted by an *ab initio* evolutionary algorithm *Phys. Rev.* B **78** 014102

[23] Ma Y, Eremets M, Oganov A R, Xie Y, Trojan I, Medvedev S, Lyakhov A O, Valle M and Prakapenka V 2009 Transparent dense sodium *Nature* **458** 182–5

[24] Oganov A R, Chen J, Gatti C, Ma Y, Ma Y, Glass C W, Liu Z, Yu T, Kurakevych O O and Solozhenko V L 2009 Ionic high-pressure form of elemental boron *Nature* **457** 863–7

[25] Ma Y, Oganov A R, Li Z, Xie Y and Kotakoski J 2009 Novel high pressure structures of polymeric nitrogen *Phys. Rev. Lett.* **102** 065501

[26] Gao G, Oganov A R, Bergara A, Martinez-Canales M, Cui T, Iitaka T, Ma Y and Zou G 2008 Superconducting high pressure phase of germane *Phys. Rev. Lett.* **101** 107002

[27] Pickard C J and Needs R J 2006 High-pressure phases of silane *Phys. Rev. Lett.* **97** 045504

[28] Martinez-Canales M, Oganov A R, Ma Y, Yan Y, Lyakhov A O and Bergara A 2009 Novel structures and superconductivity of silane under pressure *Phys. Rev. Lett.* **102** 087005

[29] Ma Y, Wang Y and Oganov A R 2009 Absence of superconductivity in the high-pressure polymorph of MgB$_2$ *Phys. Rev.* B **79** 054101

[30] Gottwald D, Likos C N, Kahl G and Löwen H 2004 Phase behavior of ionic microgels *Phys. Rev. Lett.* **92** 068301

[31] Gottwald D, Likos C N, Kahl G and Löwen H 2005 Ionic microgels as model systems for colloids with an ultrasoft electrosteric repulsion: structure and thermodynamics *J. Chem. Phys.* **122** 074903

[32] Fornleitner J, Lo Verso F, Kahl G and Likos C N 2008 Genetic algorithms predict formation of exotic configurations for two-component dipolar monolayers *Soft Matter* **4** 480

[33] Fornleitner J and Kahl G 2008 Lane formation vs. cluster formation in two dimensional square-shoulder systems—a genetic algorithm approach *Europhys. Lett.* **82** 18001

[34] Pauschenwein G J and Kahl G 2008 Clusters, columns, and lamellae—minimum energy configurations in core softened potentials *Soft Matter* **4** 1396–9

[35] Pauschenwein G J and Kahl G 2008 Zero temperature phase diagram of the square-shoulder system *J. Chem. Phys.* **129** 174107

[36] Pauschenwein G J and Kahl G 2009 Stable centered tetragonal phases in the hard core Yukawa model *J. Phys: Condens. Matter* at press

[37] Pauschenwein G J 2008 Phase behaviour of colloidal systems *PhD Thesis* Institut für Theoretische Physik, TU Wien, Austria

[38] Powell M J D 1964 An efficient method for finding the minimum of a function of several variables without calculating derivatives *Comput. J.* **7** 155–62